

## Research Article

# Inversion of Thermal Conductivity in Two-Dimensional Unsteady-State Heat Transfer System Based on Boundary Element Method and Decentralized Fuzzy Inference

Shoubin Wang <sup>1</sup>, Li Zhang,<sup>1</sup> Xiaogang Sun,<sup>2</sup> and Huangchao Jia<sup>1</sup>

<sup>1</sup>School of Control and Mechanical Engineering, Tianjin Chengjian University, Tianjin 300384, China

<sup>2</sup>School of Electrical Engineering and Automation, Harbin Institute of Technology, Harbin 150001, China

Correspondence should be addressed to Shoubin Wang; [wsbin800@126.com](mailto:wsbin800@126.com)

Received 2 January 2018; Revised 9 April 2018; Accepted 18 April 2018; Published 22 May 2018

Academic Editor: Lucia Valentina Gambuzza

Copyright © 2018 Shoubin Wang et al. This is an open access article distributed under the Creative Commons Attribution License, which permits unrestricted use, distribution, and reproduction in any medium, provided the original work is properly cited.

Based on the boundary element method and the decentralized fuzzy inference algorithm, the thermal conductivity in the two-dimensional unsteady-state heat transfer system changing with the temperature is deduced. The more accurate inversion results are obtained by introducing the variable universe method. The concrete method is as follows: using experimental means to obtain the instantaneous temperature in the material or on the boundary, to determine the thermal conductivity of the material by solving the inversion problem. The boundary element method is used to calculate the regional boundary and internal temperature in the direct problem. With the inversion problem, the decentralized fuzzy inference algorithm is used to compensate for the initial guess of the thermal conductivity by using the difference between the temperature measurement and the temperature calculation. In the inversion problem, the influence of the initial guess of different thermal conductivities, different numbers of measuring points, and the existence of measurement errors on the results is discussed. The example calculation and analysis prove that, with different initial guesses, existence of measurement errors, and the number of boundary measurements decrease, the methods adopted in this paper still maintain good validity and accuracy.

## 1. Introduction

Inversion heat transfer problems refer to the fact that some of the output information of the heat transfer system is obtained through experimental methods to invert some structural features or input information in the system. For example, the inversion of information such as the shape of the temperature boundary layer, the thermal conductivity of the material, and the heat flux density are all typical inversion heat conduction problems. Inversion heat transfer problems have been widely used in many fields such as nondestructive testing, geometrical shape optimization, aerospace engineering, power engineering, mechanical engineering, constructional engineering, bioengineering, metallurgical engineering, material processing, biological medicine, and food engineering, all of which achieve great success [1–13]. For inversion heat conduction problems, a lot of researches have been done by scholars at home and abroad.

The boundary element method and the complex variable derivation method are applied by Yu to invert the thermal conductivity of heterogeneous materials, which can effectively identify the thermal conductivity of single or multiple parameters [14]. When the heat conduction boundary value of the stability boundary is inverted by Yaparova, Laplace and Fourier transforms [15] are applied. The boundary element method is used to analyze two-dimensional transient conduction problems by Zhou et al. and the conjugate gradient method is introduced to solve the thermal conduction coefficient, which verify the effectiveness and stability of this method [16]. Mera et al. use iterative BEM to generate a stable numerical solution, which increases the number of boundary elements and reduces the amount of noise added in the input data [17]. Chen and Tanaka use a coupling application of the dual reciprocity boundary element method and dynamic programming filter to some inversion heat conduction problems [18]. A new and simple boundary element

method is presented by Gao and Wang; this method is called interface integral boundary element method for solving heat conduction problems consisting of multiple media [19]. Wang et al. apply a nonsingular indirect boundary element method for the solution of three-dimensional inversion heat conduction problems. The exact geometrical representation of computational domain is adopted by parametric equations to eliminate the errors in traditional approaches of polynomial shape functions [20].

The differential transformation is studied and a stable differential calculus method is proposed to solve the inversion heat conduction problem [21] by Baranov et al. A new method to invert the thermal conductivity of material with temperature is proposed Miao et al., by which the temperature of measurement point is obtained by finite element method, and the residual between calculated value and measured value of temperature at the measurement point is minimized to get numerical solution, proving the effectiveness and accuracy of the algorithm [22].

The thermal conductivity of material with temperature changes is piecewise discrete by temperature range by Tang et al., and the genetic algorithms and the adjoint equation are used to carry out the inversion [23] of the thermal conductivity of the full temperature range. Based on the semi-infinite one-dimensional thermal model, the thermal conductivity inversion algorithm is studied by Lei; by changing the mathematical model, different intensity of noise is simulated, and the impact of noise on the accuracy of inversion is observed and studied; the method to improve the accuracy is proposed [24].

The decentralized fuzzy inference algorithm is successfully applied to the unsteady-state heat transfer system by Ran, which shows good anti-ill-posedness and obvious advantages and effectiveness [25]. In this paper, the boundary element method is used to solve the boundary and internal temperature in the two-dimensional unsteady-state heat transfer system, and the decentralized fuzzy inference algorithm is used to compensate for the initial guess of the thermal conductivity in order to minimize the residual between the calculated and the measured values of the temperature, and the true thermal conductivity is obtained.

## 2. Direct Heat Conduction Problem

2.1. *The Boundary Integral Equation.* The mathematical model of the two-dimensional unsteady-state heat transfer problem [26]:

$$\begin{aligned} \frac{\partial^2 T}{\partial x^2} + \frac{\partial^2 T}{\partial y^2} &= \frac{1}{\alpha} \frac{\partial T}{\partial t} \quad (\in \Omega, t > t_0), \\ T &= \bar{T} \quad (\in \Gamma_1, t > t_0), \\ q &= -nk(T) \frac{\partial T}{\partial n} = \bar{q} \quad (\in \Gamma_2, t > t_0), \\ T &= T_0, \\ t &= 0. \end{aligned} \quad (1)$$

In the mathematic model formula, there are  $\Gamma_1, \Gamma_2$  and the boundary of domain  $\Omega$ , which meets  $\Gamma = \Gamma_1 + \Gamma_2$ . And  $\alpha$  is the thermal conductivity coefficient  $\alpha = k(T)/\rho c$ ,  $\rho$  is the density of the object, and  $c$  is the specific heat capacity of the object. And  $k(T)$  is the heat transfer coefficient of the object changing with temperature,  $T$  is the temperature, and  $n$  is the outer normal vector of the boundary. And  $T_f$  is the ambient temperature, and  $q$  is the heat flux density. The letter with “-” denotes the known quantity.

Weight function  $T^*$  is introduced into the expression of weighted residual of governing equation [27].

$$\begin{aligned} &\int_{t_0}^{t_1} \int_{\Omega} \left( \nabla^2 T - \frac{1}{\alpha} \frac{\partial T}{\partial t} \right) T^* d_{\Omega} d_{\tau} \\ &= \int_{t_0}^{t_1} \int_{\Gamma_2} (q - \bar{q}) T^* d_{\Gamma} d_{\tau} \\ &\quad - \int_{t_0}^{t_1} \int_{\Gamma_1} (T - \bar{T}) \frac{\partial T^*}{\partial n} d_{\Gamma} d_{\tau}. \end{aligned} \quad (2)$$

The left side of the equation is decomposed to get:

$$\begin{aligned} &\int_{t_0}^{t_1} \int_{\Omega} \left( \nabla^2 T - \frac{1}{\alpha} \frac{\partial T}{\partial t} \right) T^* d_{\Omega} d_{\tau} \\ &= \int_{t_0}^{t_1} \int_{\Omega} T^* \nabla^2 T d_{\Omega} d_{\tau} - \int_{t_0}^{t_1} \int_{\Omega} \frac{1}{\alpha} \frac{\partial T}{\partial t} T^* d_{\Omega} d_{\tau}. \end{aligned} \quad (3)$$

In Green's theorem for the Laplacian,  $\iint_D (v \nabla^2 u - u \nabla^2 v) d_{\Omega} = \int_z (v(\partial u / \partial n) - u(\partial v / \partial n)) d_s$  of which  $z$  is the boundary curve of plane closed Region  $D$  and  $d_s$  is the arc differential.

According to Laplace Green function, the following is obtained:

$$\begin{aligned} \int_{t_0}^{t_1} \int_{\Omega} \nabla^2 T T^* d_{\Omega} d_{\tau} &= \int_{t_0}^{t_1} \int_{\Gamma} \left( T^* \frac{\partial T}{\partial n} - T \frac{\partial T^*}{\partial n} \right) d_{\Gamma} d_{\tau} \\ &\quad + \int_{t_0}^{t_1} \int_{\Omega} T \nabla^2 T^* d_{\Omega} d_{\tau}. \end{aligned} \quad (4)$$

Equation (4) is taken into (3) and (2) becomes

$$\begin{aligned} &\int_{t_0}^{t_1} \int_{\Gamma} \left( T^* \frac{\partial T}{\partial n} - T \frac{\partial T^*}{\partial n} \right) d_{\Gamma} d_{\tau} + \int_{t_0}^{t_1} \int_{\Omega} T \nabla^2 T^* d_{\Omega} d_{\tau} \\ &\quad - \int_{t_0}^{t_1} \int_{\Omega} \frac{1}{\alpha} \frac{\partial T}{\partial t} T^* d_{\Omega} d_{\tau} \\ &= \int_{t_0}^{t_1} \int_{\Gamma_2} (q - \bar{q}) T^* d_{\Gamma} d_{\tau} \\ &\quad - \int_{t_0}^{t_1} \int_{\Gamma_1} (T - \bar{T}) \frac{\partial T^*}{\partial n} d_{\Gamma} d_{\tau}. \end{aligned} \quad (5)$$

It is further simplified, and  $\int_{t_0}^{t_1} \int_{\Omega} (1/\alpha)(\partial T/\partial t)T^* d_{\Omega} d_{\tau}$  is transformed to get

$$\begin{aligned} \int_{t_0}^{t_1} \int_{\Omega} \frac{1}{\alpha} \frac{\partial T}{\partial t} T^* d_{\Omega} d_{\tau} &= \int_{t_0}^{t_1} \int_{\Omega} \frac{1}{\alpha} \frac{\partial T}{\partial t} T^* d_{\Omega} d_{\tau} \\ &+ \int_{t_0}^{t_1} \int_{\Omega} \frac{1}{\alpha} \frac{\partial T^*}{\partial t} T d_{\Omega} d_{\tau} \quad (6) \\ &- \int_{t_0}^{t_1} \int_{\Omega} \frac{1}{\alpha} \frac{\partial T^*}{\partial t} T d_{\Omega} d_{\tau}. \end{aligned}$$

One Integration by parts ( $\int u dv + \int v du = uv$ ) is carried out in the equation for  $t$  to get

$$\begin{aligned} \int_{t_0}^{t_1} \int_{\Omega} \frac{1}{\alpha} \frac{\partial T}{\partial t} T^* d_{\Omega} d_{\tau} &= - \int_{t_0}^{t_1} \int_{\Omega} \frac{1}{\alpha} \frac{\partial T^*}{\partial t} T d_{\Omega} d_{\tau} \\ &+ \left[ \int_{\Omega} \frac{1}{\alpha} T^* T d_{\Omega} \right]_{t=t_0}^{t=t_1}. \quad (7) \end{aligned}$$

Equation (6) is taken into (5) to get

$$\begin{aligned} \int_{t_0}^{t_1} \int_{\Omega} T \nabla^2 T^* d_{\Omega} d_{\tau} &+ \int_{t_0}^{t_1} \int_{\Omega} \frac{1}{\alpha} \frac{\partial T^*}{\partial t} T d_{\Omega} d_{\tau} \\ &- \left[ \int_{\Omega} \frac{1}{\alpha} T^* T d_{\Omega} \right]_{t=t_0}^{t=t_1} \\ &= \int_{t_0}^{t_1} \int_{\Gamma_2} (q - \bar{q}) T^* d_{\Gamma} d_{\tau} \quad (8) \\ &- \int_{t_0}^{t_1} \int_{\Gamma_1} (T - \bar{T}) \frac{\partial T^*}{\partial n} d_{\Gamma} d_{\tau} \\ &- \int_{t_0}^{t_1} \int_{\Gamma} \left( T^* \frac{\partial T}{\partial n} - T \frac{\partial T^*}{\partial n} \right) d_{\Gamma} d_{\tau}. \end{aligned}$$

Because of  $\Gamma = \Gamma_1 + \Gamma_2$  and  $\partial T^*/\partial n = q^*$ ,  $\partial T/\partial n = q$ ,  $\int_{t_0}^{t_1} \int_{\Gamma} (T^*(\partial T/\partial n) - T(\partial T^*/\partial n)) d_{\Gamma} d_{\tau}$  is discomposed and taken into (8) to get

$$\begin{aligned} \int_{t_0}^{t_1} \int_{\Omega} T \left( \nabla^2 T^* + \frac{1}{\alpha} \frac{\partial T^*}{\partial t} \right) d_{\Omega} d_{\tau} &- \left[ \int_{\Omega} \frac{1}{\alpha} T^* T d_{\Omega} \right]_{t=t_0}^{t=t_1} \\ &= \int_{t_0}^{t_1} \int_{\Gamma_2} (q - \bar{q}) T^* d_{\Gamma} d_{\tau} - \int_{t_0}^{t_1} \int_{\Gamma_1} (T - \bar{T}) q^* d_{\Gamma} d_{\tau} \quad (9) \\ &- \int_{t_0}^{t_1} \int_{\Gamma_1 + \Gamma_2} (T^* q - T q^*) d_{\Omega} d_{\tau}. \end{aligned}$$

The corresponding basic solution to this formula is

$$T^* = \frac{1}{[4\pi\alpha(t_1 - t)]^{d/2}} \exp\left(-\frac{r^2}{4\alpha(t_1 - t)}\right), \quad (10)$$

where  $d$  is the dimensionality of space, for two-dimensional problem,  $d = 2$   $r = \sqrt{[(x - x_i)^2 + (y - y_i)^2]}$ .

Differential derivation of (10) is done to get

$$q^* = \frac{\partial T^*}{\partial n} = -\frac{D}{8\pi\alpha^2(t_1 - t)^2} \exp\left(-\frac{r^2}{4\alpha(t_1 - t)}\right). \quad (11)$$

In the formula,  $D$  is the vertical distance from the source point “ $i$ ” to the boundary element line.

The basic solution has the following characteristics:

$$\nabla^2 T^* + \frac{1}{\alpha} \frac{\partial T^*}{\partial t} = 0, \quad (12)$$

$$\int_{\Omega} T T^* d_{\Omega} = T_i(t = t_1).$$

Equations (12) and (11) are taken into (10) and a good merger of similar items is done to get

$$\begin{aligned} \frac{1}{\alpha} C_i T_i &= \int_{t_0}^{t_1} \int_{\Gamma} q T^* d_{\Gamma} d_{\tau} - \int_{t_0}^{t_1} \int_{\Gamma} T q^* d_{\Gamma} d_{\tau} \\ &+ \left[ \int_{\Omega} \frac{1}{\alpha} T^* T d_{\Omega} \right]_{t=t_0}^{t=t_1}. \quad (13) \end{aligned}$$

**2.2. The Boundary Element Equation.** The change of the function  $T$ ,  $q$  over time is small enough to be negligible compared to that of  $T^*$ ,  $q^*$ , which can be reasonably approximated as a constant over small time intervals, and (13) can be segmented into time integration [28].

$$\begin{aligned} C_i T_i + \alpha \int_{\Gamma} T \int_{t_0}^{t_1} q^* d_{\tau} d_{\Gamma} \\ &= \alpha \int_{\Gamma} q \int_{t_0}^{t_1} T^* d_{\tau} d_{\Gamma} + \left[ \int_{\Omega} T^* T d_{\Omega} \right]_{t=t_0}^{t=t_1}. \quad (14) \end{aligned}$$

And the interval integral for  $t$  is

$$\begin{aligned} \int_{t_0}^{t_1} q^* d_{\tau} &= -\frac{D}{2\pi\alpha r^2} \exp\left(-\frac{r^2}{4\alpha(t_1 - t_0)}\right), \\ \int_{t_0}^{t_1} T^* d_{\tau} &= \frac{1}{4\pi\alpha} E_i(b), \quad b = \frac{r^2}{4\alpha(t_1 - t_0)}. \quad (15) \end{aligned}$$

In the formula,  $E_i(b)$  is the exponential integral function, which can be calculated by the series, which is

$$E_i(b) = -C - \ln b + \sum_{k=1}^{\infty} (-1)^{(k-1)} \frac{b^k}{k \cdot k!}. \quad (16)$$

In the formula,  $C$  is Euler function,  $C = 0.57721566$ , for  $0 \leq b \leq 1$ ; generally the first five approximations are taken.

According to the above formula, (17) can be written as

$$\begin{aligned} C_i T_i^{t_1} + \alpha \int_{\Gamma} T^{t_1} q_t^* d_{\Gamma} &= \alpha \int_{\Gamma} q_t^{t_1} T_t^* d_{\Gamma} \\ &+ \left[ \int_{\Omega} T^* T d_{\Omega} \right]_{t=t_0}^{t=t_1}. \quad (17) \end{aligned}$$

For the spatial domain division, the boundary  $\Gamma$  is divided into  $N$  units and the domain  $\Omega$  is divided into  $M$  units. Equation (17) becomes

$$\begin{aligned} C_i T_i^{t_1} + \alpha \sum_{j=1}^N \int_{\Gamma_j} T_j^{t_1} q_t^* d\Gamma \\ = \alpha \sum_{j=1}^N \int_{\Gamma_j} q_j^{t_1} T_j^* d\Gamma + \sum_{l=1}^M \left[ \int_{\Omega_m} T^* T d\Omega \right]_{t=t_0}. \end{aligned} \quad (18)$$

Linear element interpolation is adopted and the interpolation function of linear element is  $\{\varphi_1(\xi) = (1-\xi)/2, \varphi_2(\xi) = (1+\xi)/2\}$ . Therefore, the boundary curve is approximated by a straight line. The values of  $T$  and  $q$  in the unit are approximated by the linearity with two endpoint values.

Equation (18) is done as

$$\begin{aligned} C_i T_i^{t_1} + \sum_{j=1}^N [h_{ij}^{(1)} T_j^{t_1} + h_{ij}^{(2)} T_{j+1}^{t_1}] \\ = \sum_{j=1}^N [g_{ij}^{(1)} q_j^{t_1} + g_{ij}^{(2)} q_{j+1}^{t_1}] \\ + \sum_{l=1}^M \left[ \int_{\Omega_m} T^* T d\Omega \right]_{t=t_0}. \end{aligned} \quad (19)$$

In the formula,  $\{h_{ij}^{(e)} = \alpha \int_{\Gamma_j} \varphi_e q_t^* d\Gamma, g_{ij}^{(e)} = \alpha \int_{\Gamma_j} \varphi_e T_t^* d\Gamma\}$   $e = (1, 2)$ . The formula is written in matrix form:

$$HT^{t_1} = GQ^{t_1} + P^{t_1}, \quad P = \sum_{l=1}^M \left[ \int_{\Omega_m} T^* T d\Omega \right]_{t=t_0}. \quad (20)$$

$T$  and  $q$  at the boundary node can be obtained by (21). Take  $C_i = 1$  and the inner point temperature is obtained by (13) and (18).

### 3. Decentralized Fuzzy Inversion

**3.1. Inversion of Thermal Conductivity.** The thermal conductivity inverted in this paper varies with the temperature of the material, the function of which is known. By the known measured temperature at a particular measurement point, the inversion algorithm is used to determine the constant coefficients of the function.

The difference between the temperature measurement and the temperature calculation is taken as the objective function, which is minimized as

$$J(X) = \sum_{b=1}^B \sum_{r=1}^R [T_b^{k+r-1}(X) - Y_b^{k+r-1}]^2. \quad (21)$$

$X$  is the inversion parameter in the objective function;  $T_b^{k+r-1}$  and  $Y_b^{k+r-1}$ , respectively, represent the temperature measurement and the temperature calculation at the measuring point  $T_{Cb}$  at time  $t^{k+r-1}$ ;  $B$  is the number of temperature

measuring points;  $R$  is the number of future time steps; and the minimum value of the objective function  $J(X)$  is calculated as the parameter vector  $X$  in the inversion problem.

**3.2. Decentralized Fuzzy Inference Method.** The difference between the temperature measurement and the temperature calculation is used to correspondingly compensate for the initial guess of the thermal conductivity. Therefore, a multiple-input multiple-output fuzzy inference system is established. Each independent measurement point is a single fuzzy inference unit (FIU). Fuzzy inference unit is shown in Figure 1. The independent fuzzy inference controller is divided into four parts: fuzzy interface, knowledge base, inference engine, and fuzzy decision interface (defuzzy).

The input to fuzzy inference unit  $FIU_b^r$  ( $b = 1, 2, 3, \dots, B$ ;  $r = 1, 2, 3, \dots, R$ ) is the error  $e_b^r$  of temperature calculation and measurement at the time of  $t^k, t^{k+1}, \dots, t^{k+r-1}$  at the measuring point  $T_{Cb}$  on the known boundary condition  $T_{Cb}$ :

$$e_b^r = T_b^{k+r-1}(X^k) - Y_b^{k+r-1}. \quad (22)$$

The independent fuzzy inference unit  $FIU_b^r$  output  $\Delta u_b^r$  is a fuzzy inference result corresponding to that of inputting  $e_b^r$  and is a numerical value for compensating for the guess value of the inversion parameter with only one independent measurement point  $T_{Cb}$ .

Linguistic values of each linguistic variable are defined: seven fuzzy sets are defined on the universe of inputting variable  $e_b^r$  and output variable  $\Delta u_b^r$  of  $FIU_b^r$  and these are  $\{A_1, A_2, \dots, A_7\}$  and  $\{D_1, D_2, \dots, D_7\}$ . The linguistic values corresponding to the fuzzy sets are, respectively,  $\{PB, PM, PS, ZO, NS, NM, NB\}$ . There are a lot of files and the rules are formulated flexibly and detailed. However, rules are too many and complex, and the programming is difficult, accounting for more internal storage; rare files correspond to less rules, which can be easy to implement. The disadvantage is that control function becomes less detailed, whose effect cannot be satisfactory. So setting the fuzzy rule base is to take into account both the simplicity and accuracy.

The membership function of each language value and triangle membership function are defined; the shape and distribution of membership functions are shown in Figures 2 and 3.

The knowledge base is mainly composed of two parts, the database and language control rule base. The language control rules are based on the difference between the temperature calculation and the temperature measurement. If  $e_b^r < 0$ , it is proved that the temperature calculation is smaller than the temperature measurement; it is necessary to raise the guess value of the inversion parameter to eliminate the temperature error  $e_b^r$ , and the larger the  $|e_b^r|$  is, the larger the range ability of the guess value of the inversion parameter will be. When  $e_b^r > 0$ , it is proved that the temperature calculation is larger than the temperature measurement; it is necessary to reduce the guess value of the inversion parameter to eliminate the temperature error  $e_b^r$ . The fuzzy control rules are shown in Table 1.

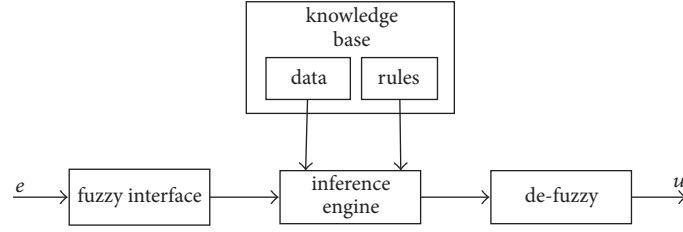


FIGURE 1: Fuzzy inference unit.

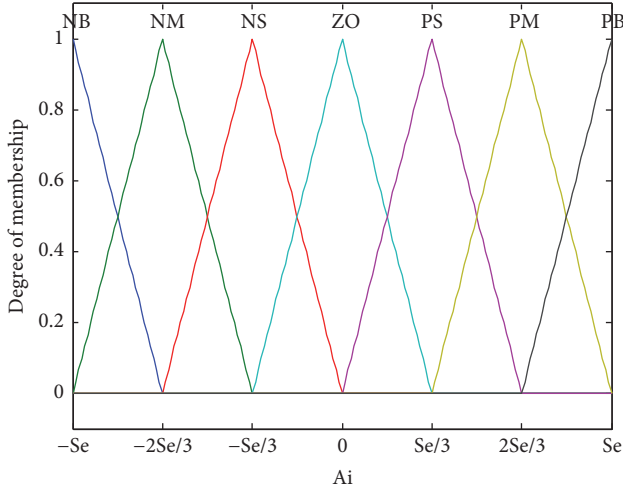


FIGURE 2: The degree of membership of fuzzy set Ai.

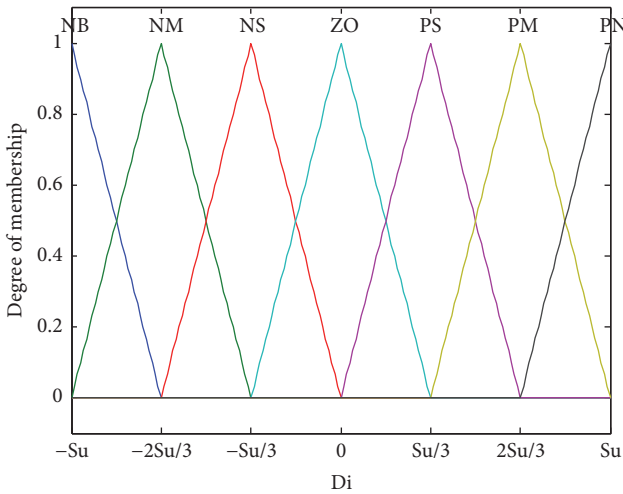


FIGURE 3: The degree of membership of fuzzy set Di.

TABLE 1: Fuzzy control rules state.

|                |    |    |    |    |    |    |    |
|----------------|----|----|----|----|----|----|----|
| $e_b^r$        | NB | NM | NS | ZO | PS | PM | PB |
| $\Delta u_b^r$ | PB | PM | PS | ZO | NS | NM | NB |

The fuzzy inference engine is based on the fuzzy input and language control rules and the fuzzy relational equation is solved to obtain the fuzzy output. Mamdani Maximum -

Minimum Fuzzy Inference Algorithm is used to determine the fuzzy set  $D$  of output variables. The set  $D$  of output variables  $\Delta u_b^r$  is from the following formula:

$$\mu_D(\Delta u_{b,0}^r) = \max_{l=1}^7 \{ \min [ \mu_{Al}(e_{b,0}^r), \mu_{Bl}(\Delta u_{b,0}^r) ] \}. \quad (23)$$

In the fuzzy decision interface, the fuzzy output is done with defuzzification to get a precise control. In the fuzzy set  $D$  output by the fuzzy inference engine, the center of gravity is used to solve defuzzification:

$$\Delta u_b^r = \frac{\int \Delta u_{b,0}^r \mu_D(\Delta u_{b,0}^r) d\Delta u_i}{\int \mu_D(\Delta u_{b,0}^r) d\Delta u_i}. \quad (24)$$

3.3. *Variable Universe.* In variable universe, the appropriate universe extension factor is to be selected; the error is changed and some changes are also made to the universe, and through the universe changing with the error changes, the precise control effect can be achieved [29, 30].

In this paper, the thermal conductivity changing with temperature is inverted; the error of the input information has a more important influence on the inversion result. Therefore, effectively reducing the sensitivity of the inversion results to the error information  $e_b^r$  is the prerequisite for obtaining a stable inversion result. Universe  $S$  increases with  $e_b^r$  decreasing, which makes the partition of universe  $S$  rough, and the corresponding output becomes more detailed. Therefore, the following variable universe formula is applied:

$$S_i = \eta \left( \frac{S}{|e_b^r|} \right)^\alpha, \quad (25)$$

in which  $[-S, S]$  is the initial input universe of  $e_b^r$ ;  $[-S_i, S_i]$  is the universe of  $e_b^r$  after being changed. In this paper, two different sets  $\eta, \alpha$  are taken based on different assumptions.

3.4. *Inversion Process.* The process of inverting thermal conductivity is as follows.

(1) Set the number of iterations  $h = 0$  and take the initial guess of thermal conductivity  $X$ .

(2) Calculate the direct problem to get temperature calculation at the temperature at point  $b$ .

(3) From (23), the deviation  $e_b^r$  can be calculated to determine whether the convergence condition  $J(q) \leq \varepsilon$  is satisfied. If it is satisfied, the iteration is stopped. The value  $X$  is assumed to be the thermal conductivity; otherwise, the next calculation is performed.

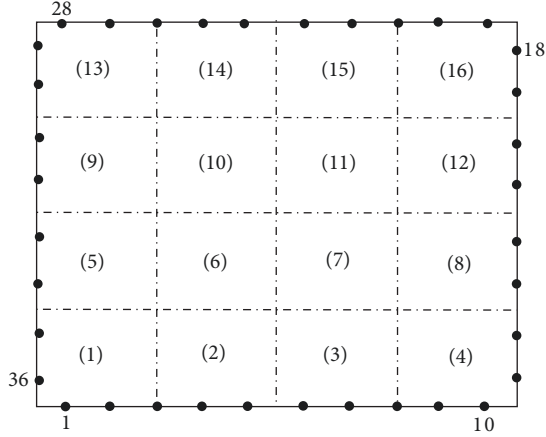


FIGURE 4: Schematic diagram.

- (4) Calculate the real-time universe  $[-S_i, S_i]$  from (25).
- (5) Determine  $\Delta u_b^r$  by one-dimensional fuzzy inference unit FIU<sub>i</sub>.
- (6) Calculate the new guess of thermal conductivity  $X^{h+1}$  and return to step (2).

#### 4. The Instance Calculation and Analysis

The schematic diagram is shown in Figure 4. A transient heat conduction problem in a  $10 \times 8$  quadrilateral region is considered and the thermal conductivity meets

$$K(T) = K_0 + \lambda(T - T_0). \quad (26)$$

$T_0$  is the initial temperature,  $K_0$  is the thermal conductivity at temperature  $T_0$ , and  $\lambda$  is an experimentally determined constant. For simplicity of description, the physical properties of the material are set to  $\rho = 1$   $c = 1$ . The temperature of the four boundaries is  $1^\circ\text{C}$ , the initial temperature in the domain is  $0^\circ\text{C}$ , the boundary is divided into 36 boundary elements, and the domain is divided into 16 quadrilateral elements. The material thermal conductivity inversion is done under the premise of the temperature at the measuring point in the domain is known. The function of thermal conductivity is known,  $K_0 = 1$   $\lambda = 1/10$ , the correct thermal conductivity is introduced into the direct problem to get the temperature at the measuring point at different time, and the correct temperature is defined as the temperature measurement. In the inversion process  $K(T)$ ,  $T$  is the temperature at this position at the previous moment. The number of measuring points is selected as  $B \in \{3, 6, 9\}$ , at each measuring four point temperature calculations of different time are taken, and by inversion the three groups of data of the temperature and the corresponding thermal conductivity are obtained.

When there is a measurement error, temperature measurement at the measuring point is

$$Y_b^{k+r-1} = Y_b^{k+r-1} + \omega\sigma. \quad (27)$$

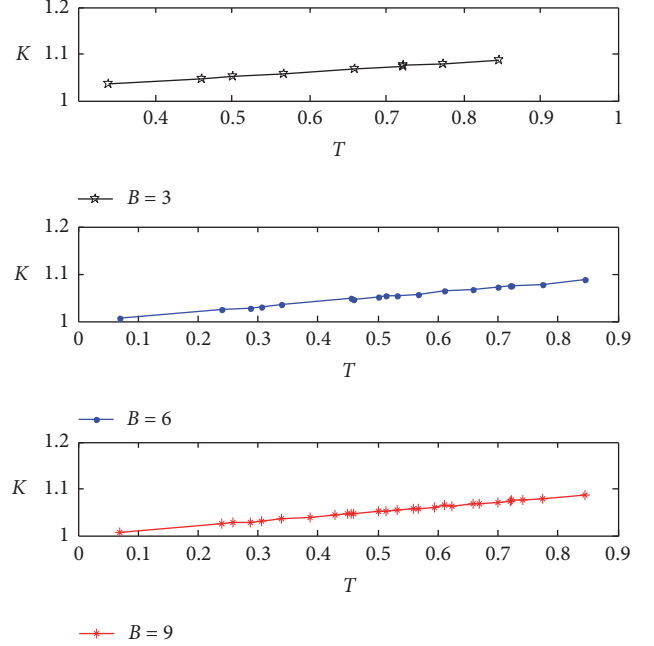


FIGURE 5: The inversion result of the thermal conductivity.

In this formula,  $\omega$  is the random number of the normal distribution  $N(0, 0.01)$  and  $\sigma$  is the standard deviation of the measurement.

**4.1. The Impact of the Number of Measuring Points.** The initial guess value is taken as  $K(T) = 1.5$ , the standard deviation of measurement is taken as  $\sigma = 0$ , the number of temperature measurement points is taken as  $B = 3, B = 6, B = 9$ , and the temperature at the measuring point and the corresponding thermal conductivity are obtained by inversion. The inversion result is shown in Figure 5.

At the measuring point  $B = 3, B = 6, B = 9$ , by the least square method  $K_0$  and  $\lambda$  are calculated, and the average relative errors are shown in Table 2. When  $B = 3$ , the average relative errors of  $K_0$  and  $\lambda$  are 0.28% and 3.5%; when  $B = 6$ , the average relative errors of  $K_0$  and  $\lambda$  are 0.14% and 3.0%, respectively; when  $B = 9$ , the average relative errors of  $K_0$  and  $\lambda$  are 0.05% and 2.1%, respectively. And thus it is shown that, by increasing the number of measuring points, the average relative error decreases and the inversion accuracy improves.

**4.2. The Impact of Initial Guess.** The number of measuring points is  $B = 9$ , the standard deviation of measurement is  $\sigma = 0$ , and three different initial guesses,  $K(T) = 1, K(T) = 1.5$ , and  $K(T) = 2.0$  are used, respectively, for numerical test. The inversion result is shown in Figure 6.

$K(T) = 1, K(T) = 1.5$ , and  $K(T) = 2.0$  are used, respectively, by the least square method to calculate the value of  $K_0$  and  $\lambda$ ; the average relative errors are shown in Table 3. When  $K(T) = 1$ , the average relative errors of  $K_0$  and  $\lambda$  are 0.02% and 4.4%; when  $K(T) = 1.5$ , the average relative errors of  $K_0$  and  $\lambda$  are 0.05% and 2.1%; when  $K(T) = 2.0$ , the average relative errors of  $K_0$  and  $\lambda$  are 0.06% and 3.0%. It can be seen

TABLE 2: The value of  $K_0$ ,  $\lambda$  and the average relative error.

| Test points | Calculated value of $K_0$ | Calculated value of $\lambda$ | Relative error of $K_0$ (%) | Relative error of $\lambda$ (%) |
|-------------|---------------------------|-------------------------------|-----------------------------|---------------------------------|
| 3           | 0.9972                    | 0.1035                        | 0.28                        | 3.5                             |
| 6           | 0.9986                    | 0.1030                        | 0.14                        | 3.0                             |
| 9           | 0.9995                    | 0.1021                        | 0.05                        | 2.1                             |

TABLE 3: The value of  $K_0$ ,  $\lambda$  and the average relative error.

| Hypothetical value | Calculated value of $K_0$ | Calculated value of $\lambda$ | Relative error of $K_0$ (%) | Relative error of $\lambda$ (%) |
|--------------------|---------------------------|-------------------------------|-----------------------------|---------------------------------|
| 1                  | 1.0002                    | 0.0966                        | 0.02                        | 4.4                             |
| 1.5                | 0.9995                    | 0.1021                        | 0.05                        | 2.1                             |
| 2.0                | 1.0006                    | 0.1030                        | 0.06                        | 3.0                             |

TABLE 4: The value of  $K_0$ ,  $\lambda$  and the average relative error.

| $\sigma$ Standard deviation | Calculated value of $K_0$ | Calculated value of $\lambda$ | Relative error of $K_0$ (%) | Relative error of $\lambda$ (%) |
|-----------------------------|---------------------------|-------------------------------|-----------------------------|---------------------------------|
| $\sigma = 0$                | 0.9995                    | 0.1021                        | 0.05                        | 2.1                             |
| $\sigma = 0.2$              | 0.9980                    | 0.0970                        | 0.20                        | 3.0                             |
| $\sigma = 0.4$              | 0.9860                    | 0.1361                        | 1.4                         | 36.1                            |

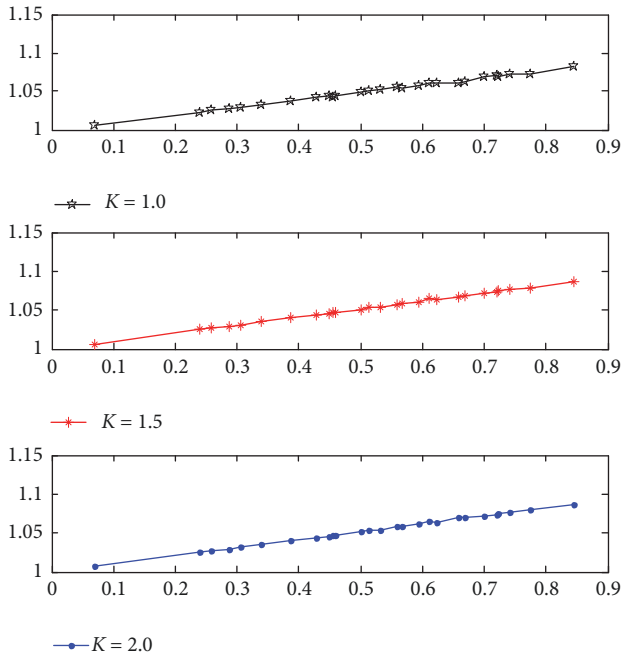


FIGURE 6: The inversion result of the thermal conductivity.

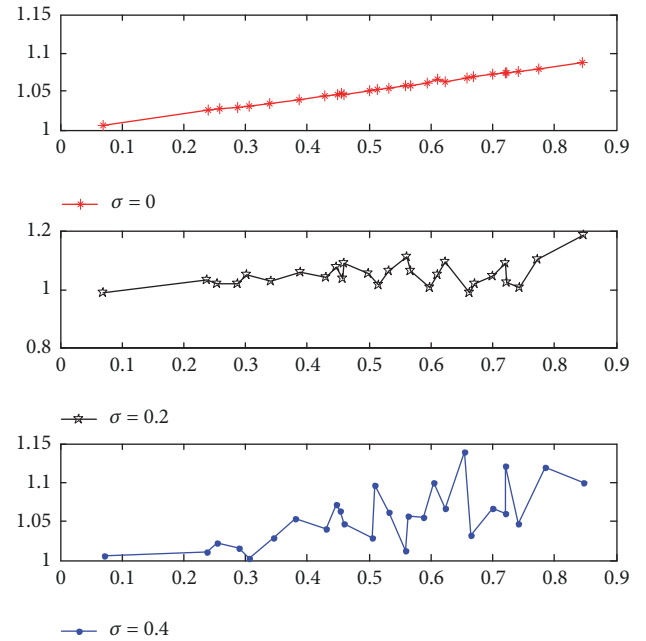


FIGURE 7: The inversion result of the thermal conductivity.

that the initial guess has a certain effect on the result, but the satisfactory result can be obtained within a reasonable range.

**4.3. The Impact of Measurement Error.** The initial guess is  $K(T) = 1.5$ , the number of measuring points is  $B = 9$ , and three groups of standard deviation,  $\sigma = 0$ ,  $\sigma = 0.2$ ,  $\sigma = 0.4$  are used, respectively, for numerical test. The inversion result is shown in Figure 7.

The standard deviations of measurement are  $\sigma = 0$ ,  $\sigma = 0.2$ ,  $\sigma = 0.4$ ; the values of  $K_0$ ,  $\lambda$  are calculated by the

least square method; the average relative errors are shown in Table 4. When  $\sigma = 0$ , the average relative errors of  $K_0$  and  $\lambda$  are 0.05% and 2.1%; when  $\sigma = 0.2$ , the average relative errors of  $K_0$  and  $\lambda$  are 0.20% and 3.0%; when  $\sigma = 0.4$ , the average relative errors of  $K_0$  and  $\lambda$  are 1.40% and 36.1%. It can be seen that there are some measurement errors under the premise of large amount of measurement data, and the inversion results can still be satisfactory. However, the larger the standard deviation of measurement is, the more distorted the inversion results will be.

## 5. Conclusion

In this paper, the boundary element method and decentralized fuzzy inference algorithm are used to invert the thermal conductivity changing with temperature in two-dimensional unsteady-state heat transfer system. The effects of initial guess, different number of measuring points, and measurement errors on the results are discussed. It proves that if the initial guess is taken within a reasonable range and when there is some measurement error, inversion results can be satisfactory. Through the calculation and analysis of examples, the accuracy and stability of the thermal conductivity inversion algorithm are verified.

## Data Availability

In order to better share our research results, we agree to distribute the data publicly. The data relating to this research is available upon request by contacting the corresponding author, Shoubin Wang (wsbin800@126.com, +86-022-23773022).

## Disclosure

The founding sponsors had no role in the design of the study; in the collection, analyses, or interpretation of data; in the writing of the manuscript; and in the decision to publish the results.

## Conflicts of Interest

The authors declare no conflicts of interest.

## Authors' Contributions

Shoubin Wang and Li Zhang proposed mathematical description of boundary element method; Xiaogang Sun proved the decentralized fuzzy inference method; Li Zhang and Huangchao Jia designed the experiments and analyzed the results. Li Zhang wrote part of code.

## Acknowledgments

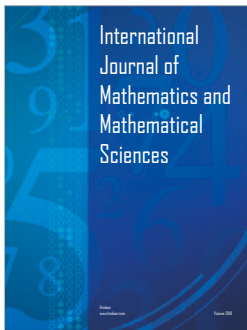
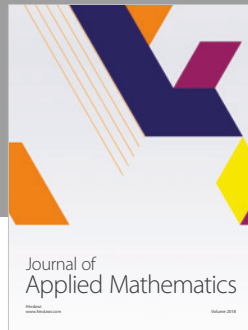
This work was financially supported by the National Key Foundation for Exploring Scientific Instrument of China (2013YQ470767), Tianjin Science and Technology Committee for Science and Technology Development Strategy Research Project (15ZLZLZF00350), Tianjin Science and Technology Commissioner Project (16JCTPJC53000), and the 13th Five-Year Plan (2016–2020) of Science Education Project in Tianjin City (HE1017).

## References

- [1] S. Wang, L. Zhang, X. Sun, and H. Jia, "Solution to two-dimensional steady inverse heat transfer problems with interior heat source based on the conjugate gradient method," *Mathematical Problems in Engineering*, vol. 2017, Article ID 2861342, 9 pages, 2017.
- [2] C. Sheng, *Direct and Inverse Heat Conduction Problems Solving By the Boundary Element Method*, Hunan University, 2007.
- [3] F. Mohebbi, M. Sellier, and T. Rabczuk, "Estimation of linearly temperature-dependent thermal conductivity using an inverse analysis," *International Journal of Thermal Sciences*, vol. 117, pp. 68–76, 2017.
- [4] K. A. Woodbury, J. V. Beck, and H. Najafi, "Filter solution of inverse heat conduction problem using measured temperature history as remote boundary condition," *International Journal of Heat and Mass Transfer*, vol. 72, pp. 139–147, 2014.
- [5] P. Duda, "Numerical and experimental verification of two methods for solving an inverse heat conduction problem," *International Journal of Heat and Mass Transfer*, vol. 84, pp. 1101–1112, 2015.
- [6] S. Jiang, Z. Zhenyu et al., "Geometry estimation of furnace inner wall based on bem and decentralized fuzzy inference method," *World journal of science and technology: ROAD*, vol. 2, pp. 122–126, 2015.
- [7] F. Bozzoli, A. Mocerino, and S. Rainieri, "Inverse heat transfer modeling applied to the estimation of the apparent thermal conductivity of an intumescent fire retardant paint," *Experimental Thermal & Fluid Science*, p. 90, 2017.
- [8] D. Xu and P. Cui, "Simultaneous determination of thickness, thermal conductivity and porosity in textile material design," *Journal of Inverse and ILL-Posed Problems*, vol. 24, no. 1, pp. 59–66, 2016.
- [9] J. Zhao, Z. Fu, X. Jia, and Y. Cai, "Inverse determination of thermal conductivity in lumber based on genetic algorithms," *Holzforschung*, vol. 70, no. 3, pp. 235–241, 2016.
- [10] Z. Jingsheng, *Development of Device for Measuring Thermal Conductivities*, Harbin Institute of Technology, 2016.
- [11] M. Arghand and M. Amirfakhrian, "A meshless method based on the fundamental solution and radial basis function for solving an inverse heat conduction problem," *Advances in Mathematical Physics*, vol. 2015, Article ID 256726, 8 pages, 2015.
- [12] L. Gosselin, M. Tye-Gingras, and F. Mathieu-Potvin, "Review of utilization of genetic algorithms in heat transfer problems," *International Journal of Heat and Mass Transfer*, vol. 52, no. 9–10, pp. 2169–2188, 2009.
- [13] H.-L. Lee, W.-J. Chang, W.-L. Chen, and Y.-C. Yang, "Inverse heat transfer analysis of a functionally graded fin to estimate time-dependent base heat flux and temperature distributions," *Energy Conversion and Management*, vol. 57, no. 2, pp. 1–7, 2012.
- [14] Y. Xiaochun, *Inverse Analysis of Thermal Conductivities in Non-Homogeneous Heat Conductions Using Boundary Element Method*, Dalian University of Technology, 2013.
- [15] N. Yaparova, "Numerical methods for solving a boundary-value inverse heat conduction problem," *Inverse Problems in Science and Engineering*, vol. 22, no. 5, pp. 832–847, 2014.
- [16] Z. Huanlin, X. Xingsheng et al., "Identification of temperature-dependent thermal conductivity for 2-D transient heat conduction problems," *Applied Mathematics and Mechanics*, vol. 12, no. 35, pp. 1341–1351, 2014.
- [17] N. S. Mera, L. Elliott, D. B. Ingham, and D. Lesnic, "Iterative boundary element method for solving the one-dimensional backward heat conduction problem," *International Journal of Heat and Mass Transfer*, vol. 44, no. 10, pp. 1937–1946, 2001.
- [18] W. Chen and M. Tanaka, "Solution of some inverse heat conduction problems by the dynamic programming filter and BEM," *Inverse Problems in Engineering Mechanics III*, pp. 23–28, 2002.



- [19] X.-W. Gao and J. Wang, "Interface integral BEM for solving multi-medium heat conduction problems," *Engineering Analysis with Boundary Elements*, vol. 33, no. 4, pp. 539–546, 2009.
- [20] F. Wang, W. Chen, W. Qu, and Y. Gu, "A BEM formulation in conjunction with parametric equation approach for three-dimensional Cauchy problems of steady heat conduction," *Engineering Analysis with Boundary Elements*, vol. 63, pp. 1–14, 2016.
- [21] V. L. Baranov, A. A. Zasyad'ko, and G. A. Frolov, "Integro-differential method of solving the inverse coefficient heat conduction problem," *Journal of Engineering Physics and Thermophysics*, vol. 83, no. 1, pp. 60–71, 2010.
- [22] C. Miao, G. Xiaowei et al., "Inversion of temperature-dependent thermal conductivity based on transient inverse heat conduction problems," *Proceedings of the CSEE*, vol. 32, pp. 82–87, 2012.
- [23] T. Zhonghua, Q. Guohong et al., "Estimation of temperature-dependent function of thermal conductivity for a material," *Chinese Journal of Computational Mechanics*, vol. 28, no. 3, pp. 377–382, 2011.
- [24] C. Lei, *Research on Inversion Algorithms of Thermo Physical Properties*, Harbin Institute of Technology, 2015.
- [25] R. Wen, "Research on fuzzy Inference method based on variable universe for transient Inverse heat transfer problems," 2017.
- [26] P. Duda, "A method for transient thermal load estimation and its application to identification of aerodynamic heating on atmospheric reentry capsule," *Aerospace Science and Technology*, vol. 51, pp. 26–33, 2016.
- [27] S. Wang, H. Jia, X. Sun, and L. Zhang, "Two-dimensional steady-state boundary shape inversion of CGM-SPSO algorithm on temperature information," *Advances in Materials Science and Engineering*, vol. 2017, Article ID 2461498, 12 pages, 2017.
- [28] W. Hongtan, *Conduction Problem Solving By Boundary Element Method*, National Defence Industry Press, Beijing, China, 2008.
- [29] P. Xiangfei and S. Lizhong, "Effectiveness of several shrinkage factors of variable universe fuzzy contro," *Control Engineering of China*, vol. s2, pp. 106–108, 2008.
- [30] G. Haigang, *Several Novel Methods of Variable Universe Adaptive Fuzzy Control*, Dalian University of Technology, 2013.



**Hindawi**

Submit your manuscripts at  
[www.hindawi.com](http://www.hindawi.com)

